

Thermal characterization of Al₂O₃ and ZnO reinforced silicone rubber as thermal pads for heat dissipation purposes

L.C. Sim^{a,*}, S.R. Ramanan^a, H. Ismail^a, K.N. Seetharamu^b, T.J. Goh^c

^a School of Materials and Mineral Resources Engineering, University Sains Malaysia, 14300 Nibong Tebal, Penang, Malaysia

^b School of Mechanical Engineering, Universiti Sains Malaysia, 14300 Nibong Tebal, Penang, Malaysia

^c Intel Technology Sdn. Bhd., Bayan Lepas Industrial Zone, Phase 3, Halaman Kampung Jawa, 11900 Penang, Malaysia

Received 8 July 2004; received in revised form 11 December 2004; accepted 30 December 2004

Available online 16 February 2005

Abstract

Silicone rubber filled with thermally conductive, but electrically insulating Al₂O₃ or ZnO fillers were investigated to be used as elastomeric thermal pads, a class of thermal interface materials. The effect of Al₂O₃ or ZnO fillers on the thermal conductivity and coefficient of thermal expansion (CTE) of the silicone rubber were investigated, and it was found that with increasing Al₂O₃ or ZnO fillers, the thermal conductivity of the thermal pads increases, while the coefficient of thermal expansion (CTE) decreases. The thermal conductivity results obtained were also analyzed using the Agari model to explain the effect of Al₂O₃ or ZnO fillers on the formation of thermal conductive networks. Thermal gravimetry analysis (TGA) showed that the addition of either Al₂O₃ or ZnO fillers increases the thermal stability of the silicone rubber, while the scanning electron microscope (SEM) showed that at 10 vol.% filler loading percolation threshold has yet to be reached.

© 2005 Elsevier B.V. All rights reserved.

Keywords: Thermal interface materials; Silicone rubber; Elastomeric thermal pads; Heat dissipation

1. Introduction

Recent advancement in electronics technology has resulted in the miniaturization of transistors, allowing more transistors to be crammed and integrated into a single device, resulting in a higher performance device [1]. Nevertheless, integration and cramming of transistors has resulted in the escalation of power dissipation as well as an increase in heat flux at the devices. It is well known that the reliability of devices is exponentially dependant on the operating temperature of the junction, whereby a small difference in operating temperatures (in the order of 10–15 °C) can result in a two times reduction in the lifespan of a device [2]. Therefore, it is essentially crucial for the heat generated from the devices to be dissipated as quickly and effectively as possible, to maintain the operating temperatures of the device at a desired level [3,4].

Among the various methods used to dissipate heat from the devices includes the attachment of a high thermal conductivity and low coefficient of thermal expansion (CTE) heat sink or heat spreader on the devices [5–7]. However, without good thermal contacts, the performance of a high thermal conductivity heat sink to dissipate heat is limited, due to interfacial thermal resistance arising from non-surface flatness and surface roughness of both the devices and heat sink. Non-surface flatness, are commonly observed in the form of convex, concave and wavy surfaces, resulting in as much as 99% of the interfaces being separated by air gaps [8]. Interstitial air gaps trapped due to improper mating of the surfaces significantly reduces the capability to dissipate heat, due to the low thermal conductivity value of air ($k_{\text{air}} = 0.026 \text{ Wm}^{-1} \text{ K}^{-1}$). One method that is commonly used to reduce the thermal contact resistance between the two surfaces is to include an additional material, commonly referred as thermal interface materials (TIM), to provide an effective heat path, as shown in Fig. 1 [9–14].

* Corresponding author. Tel.: +60 4 5941010; fax: +60 4 5941011.
E-mail address: lcsim78@hotmail.com (L.C. Sim).

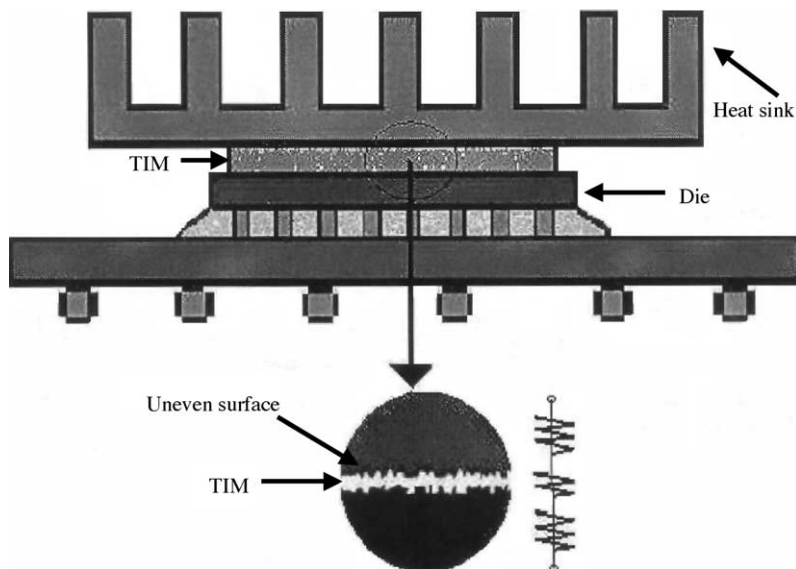


Fig. 1. Surface roughness between heat sink and device filled with TIM.

TIMs are typically made up of polymer or silicone matrix reinforced with highly thermally conductive but electrical insulating fillers such as aluminum nitride, boron nitride, alumina or silicon carbide [15–17]. An ideal TIM should not only have high thermal conductivity but must also have low coefficient of thermal expansion. Besides that the material must be easily deformed by small contact pressure to contact all the uneven areas of the mating surfaces [15].

TIMs can be categorized into elastomeric thermal pads, thermal greases, solders and phase change materials [18,19]. Of all the classes of TIMs mentioned, elastomeric thermal pads are popular for cooling of low power devices, such as chip sets and mobile processors [2]. Elastomeric thermal pads, typically 200–1000 μm thick, consists of elastomer filled with either ceramic or metal fillers. The advantages of elastomeric thermal pads is that they are easy to handle, in addition to being compressible to 25% of their total thickness, enabling the pads to absorb tolerance variances in assemblies [2].

In this study, elastomeric thermal pads were developed from silicone rubber filled with alumina (Al_2O_3) or zinc oxide (ZnO) fillers at various loadings up to 10 vol.%. Filler loading in the present study has been limited to 10 vol.% to avoid the hardening of pads, which could consequently result in an increase in contact resistance. The effect of Al_2O_3 or ZnO fillers at various filler loadings on the thermal conductivities and coefficient of thermal expansion (CTE) of the silicone rubber were studied. Experimental data obtained was fitted into a model equation, namely Maxwell–Eucken, Bruggeman, Cheng–Vochan and Agari for thermal conductivity and rules of mixture for CTE, with the values obtained, analyzed and compared. The developed thermal pads were also investigated for thermal stability using the thermal gravimetry analysis (TGA).

2. Experimental

2.1. Materials

Silicone rubber used in this study, is a siloxane based polymer manufactured by Shin–Etsu silicones, while the curing agent used was 2,5-bis(*tert*-butyl peroxy)-2,5-dimethylhexane, also from Shin–Etsu silicones. All the above chemicals are used as received. The fillers used in this study are aluminium oxide (Al_2O_3) 99.9% and zinc oxide (ZnO) 99.7% from Aldrich, with an average particle size of 10 and 1 μm , respectively. Silicone rubber was chosen as the matrix for the thermal pads due to the thermo-stability, and chemical inertness of the silicone rubber [20–23], while Al_2O_3 and ZnO were investigated due to their low CTE and high thermal conductivity properties. The property of the materials used is shown in Tables 1 and 2.

Table 1
Properties of Al_2O_3 and ZnO fillers

Fillers	Al_2O_3	ZnO
Mean particle size (μm)	10	1
Density (g/cm^3)	4.000	5.610
CTE ($10^{-6} \text{ }^\circ\text{C}^{-1}$)	7.4	2.0
Thermal conductivity ($\text{Wm}^{-1} \text{ K}^{-1}$)	30	60
Bulk modulus (GPa)	247	134
Shear modulus (GPa)	158	44

Table 2
Properties of silicone rubber

Density (g/cm^3)	1.07
CTE ($10^{-6} \text{ }^\circ\text{K}^{-1}$)	300
Thermal conductivity ($\text{Wm}^{-1} \text{ K}^{-1}$)	0.18–0.2
Dielectric constant	2.6–6.3
Tensile strength (MPa)	1.57–30

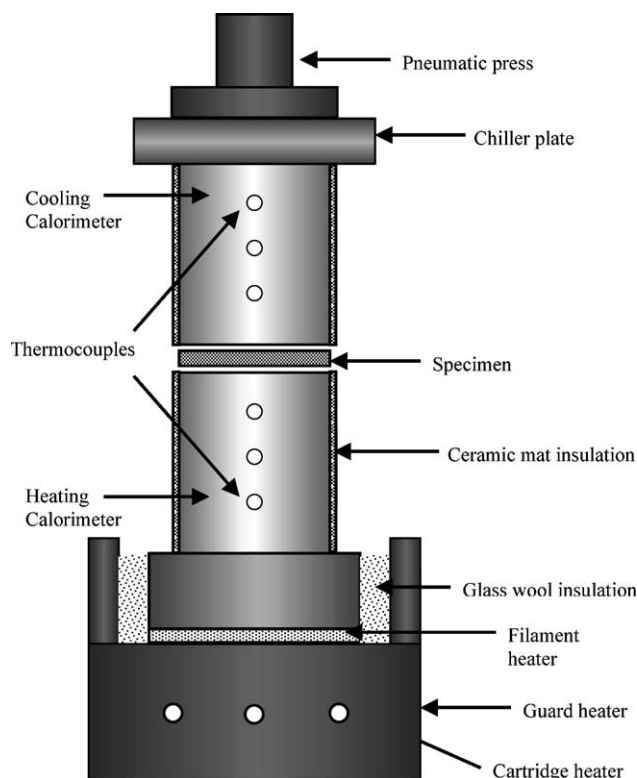


Fig. 2. Schematic diagram of the guarded heater meter (based on ASTM D5470).

2.2. Sample preparation

Silicone rubber was first compounded with peroxide catalyst, followed by the addition of Al_2O_3 or ZnO fillers. The compounding was carried out on a laboratory size (160 mm diameter \times 320 mm length) two roll mixing mill, in accordance with the ASTM D3184-80 [24] (Fig. 2). The total mixing time for all the different concentrations (2, 4, 6, 8, 10 vol.%) were kept at 15 min and the temperature of mixing (26°C) was maintained constant by circulating cold water through the rollers. The optimum cure time (t_{90}) of each sample was determined at 150°C from the Monsanto Rheometer, model MDR 2000, and are listed in Table 3. Finally the sam-

Table 3
Cure time of silicone rubber compounds with Al_2O_3 or ZnO fillers at various volume fractions

Fillers	Fillers (vol.%)	Cure time (t_{90}) (min)
Al_2O_3	0	15.61
	2	8.98
	4	8.80
	6	8.69
	8	8.67
	10	8.65
ZnO	2	8.78
	4	9.02
	6	9.47
	8	9.69
	10	9.71

ples were compression molded at 150°C in an electrically heated hot press based on their respective cure times to form 0.2 mm thick thermal pads. For this a 0.2 mm thick stainless steel mold was used, and the samples were compressed under a pressure of 100 psi.

2.3. Characterization

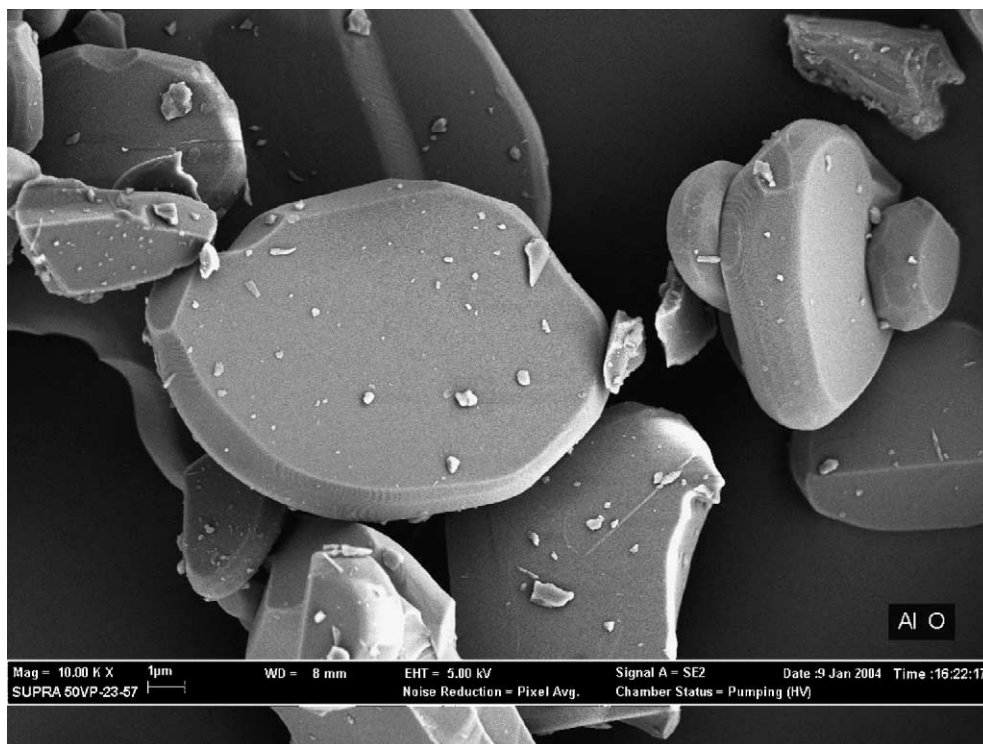
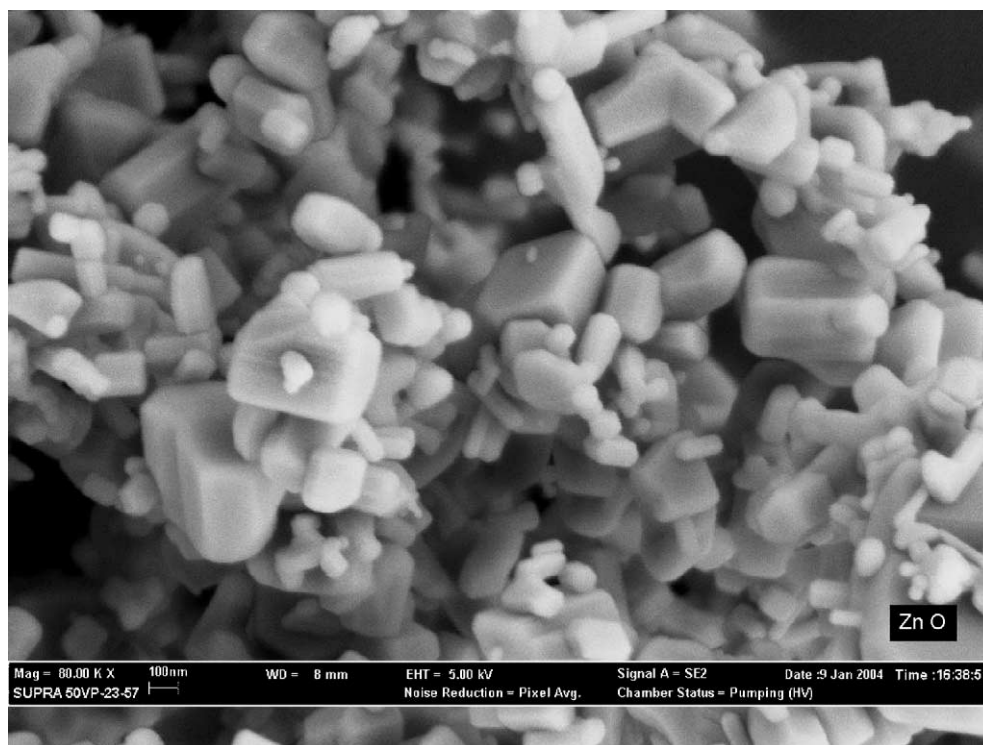
Morphological observations on the thermal pads were done using the scanning electron microscope (SEM), Model Cambridge Stereoscan 200. Observations were carried out on the cross-section of both the Al_2O_3 and ZnO filled thermal pads, to study the filler distribution and morphology which is known to affect the thermal conductivity of the thermal pads.

Weight loss of the elastomeric thermal pads upon heating was measured using the Perkin-Elmer TGA7 Thermogravimetric analyzer. Measurements were conducted in an air atmosphere, from room temperature to 250°C , at a heating rate of $5^\circ\text{C}/\text{min}$. The observed weight loss was analyzed.

CTE measurements of the Al_2O_3 and ZnO filled thermal pads were measured using the Perkin-Elmer TMA-7 system. The samples for CTE measurements are (2 mm \times 2 mm \times 0.2 mm) in size and were prepared from the hot pressed thermal pads. The samples were then mounted on the TMA and heated from 30 to 250°C at a heating rate of $5^\circ\text{C}/\text{min}$. During the measurements, a small loading force of 5 mN was applied to reduce the induced deformation. Coefficient of thermal expansion was determined from the slope of thermal expansion versus temperature.

Thermal conductivity ($\text{Wm}^{-1}\text{K}^{-1}$) of the thermal pads was measured using the guarded heater meter apparatus (Fig. 2), which was fabricated according to the ASTM D-5470 [25]. This method was chosen over the novel flash method, as it is more suitable for analyzing materials with temperature sensitive thermal and mechanical properties. Most importantly additional materials properties, such as density and heat capacity that introduces additional sources of error are not needed in the measurement [26].

Thermal conductivity measurements were carried out on thermal pads with a dimension of (1.2 mm \times 1.2 mm \times 0.2 mm) in size, cut from the hot pressed thermal pads. Measurements were carried out by heating the heater blocks up to 100°C , with the thermal pads clamped in between the two calorimeters in order to produce an average specimen temperature of 50°C [25]. For this, a chiller plate with circulating water at a temperature of 26°C was placed above the cooling calorimeter to create a thermal gradient from the heating calorimeter to the cooling calorimeter. During measurements, an onset pressure of 1 bar was applied to reduce the effects of contact resistance between the specimen and the calorimeters due to minor surface irregularities. Readings from the thermocouples are recorded when equilibrium is achieved, whereby two

Fig. 3. SEM micrograph of aluminium oxide (Al_2O_3).Fig. 4. SEM micrograph of zinc oxide (ZnO).

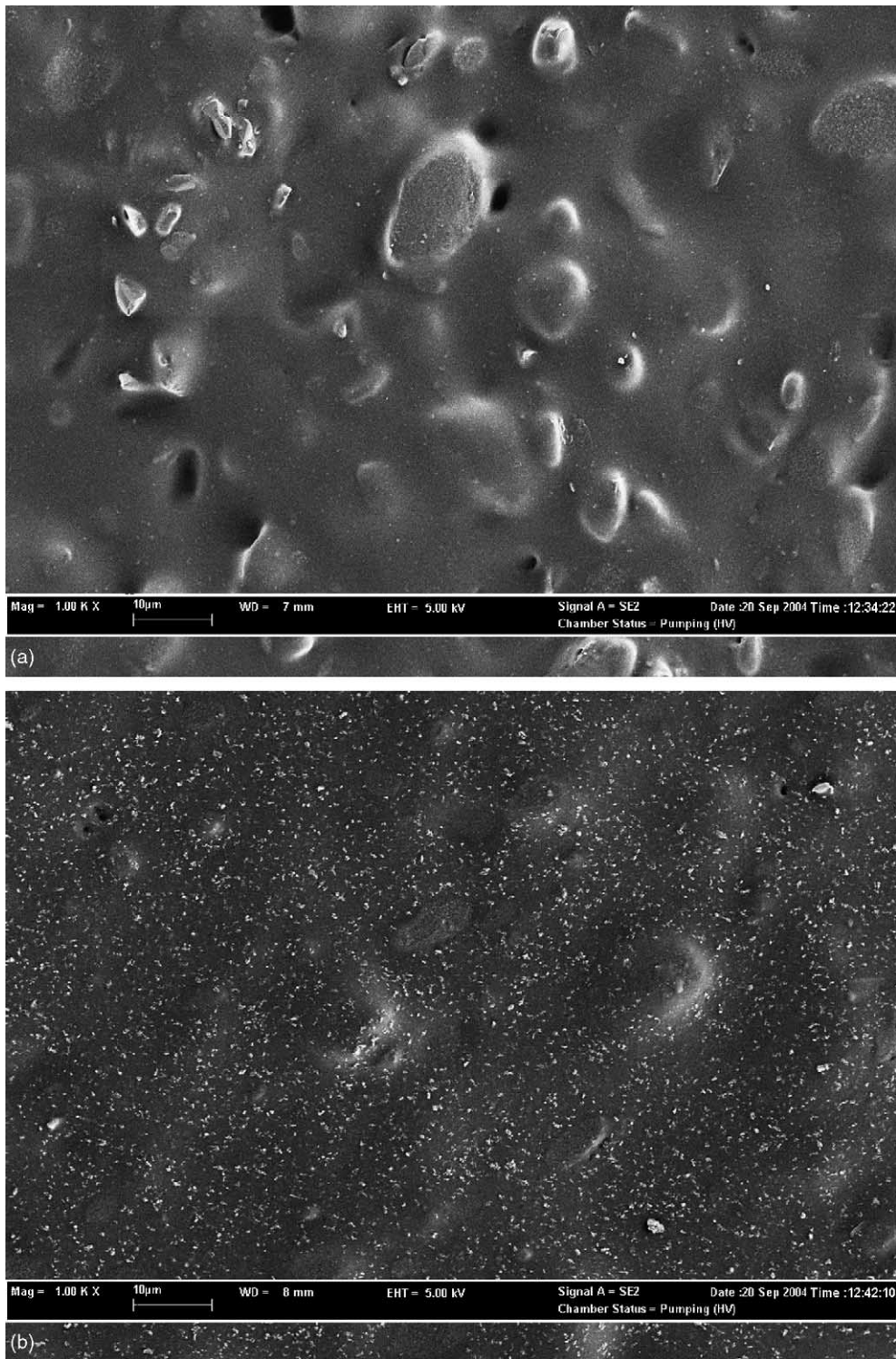


Fig. 5. (a) Cross section of 10 vol.% Al_2O_3 filled thermal pads (1000 \times); (b) cross section of 10 vol.% ZnO filled thermal pads (1000 \times).

successive set of temperature readings are taken at 15 min interval, shows a difference of $\pm 0.1^\circ\text{C}$.

The thermal conductivity of the thermal pads were calculated from the Fourier's law, as is shown in Eq. (1), based on the assumption that the heat flow is one dimensional in the perpendicular direction, and no heat loss occurs in the lateral

direction:

$$k_{\text{TIM}} = \frac{Q\Delta L}{A[T_{\text{hot.int}} - T_{\text{cold.int}}]} \quad (1)$$

where k is the thermal conductivity of thermal pads ($\text{Wm}^{-1}\text{K}^{-1}$), Q the average heat flux generated by the

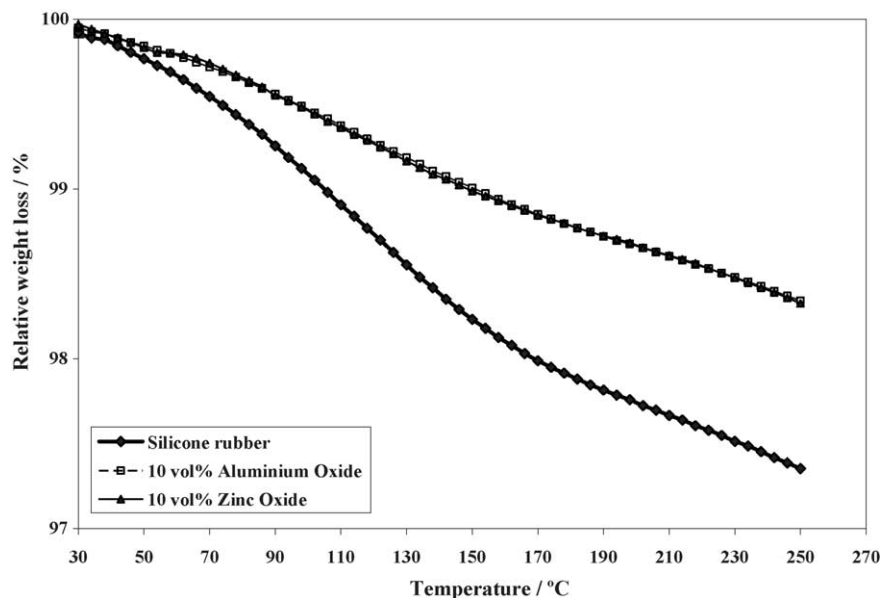


Fig. 6. Comparison between the thermal stability of unfilled silicone rubber with Al_2O_3 and ZnO filled silicone rubber.

cartridge heaters (W), $T_{\text{hot.int}}$ the interface temperature of the heating calorimeter (K), $T_{\text{cold.int}}$ the interface temperature of the cooling calorimeter (K), A the surface area of tested thermal pads (m^2), and ΔL the thickness of thermal pads (m).

The average heat flux (Q) is the amount of heat generated by two cartridge heaters, while the interface temperature for both the heating and cooling calorimeter were extrapolated from the temperature gradients obtained from the three thermocouples embedded in each of the calorimeter block. The thicknesses of the thermal pads (ΔL) were measured using a digital camera, with pin guides embedded in the calorimeter blocks as guidelines.

3. Results and discussion

3.1. Morphology observations

The state of filler distribution is important, as under the percolation theory; filler units need to touch one another to form a continuous heat conduction path [27,28]. SEM micrographs of the Al_2O_3 (Fig. 3) and ZnO fillers (Fig. 4), showed that Al_2O_3 fillers have a flat platelet shape, while ZnO fillers are rhombohedral in shape. Fig. 5(a) is a SEM micrograph showing the cross-section of the Al_2O_3 filled thermal pads while Fig. 5(b) is that of ZnO filled thermal pads. Both the samples are at 10 vol.% filler loading. From Fig. 5(a) and (b)

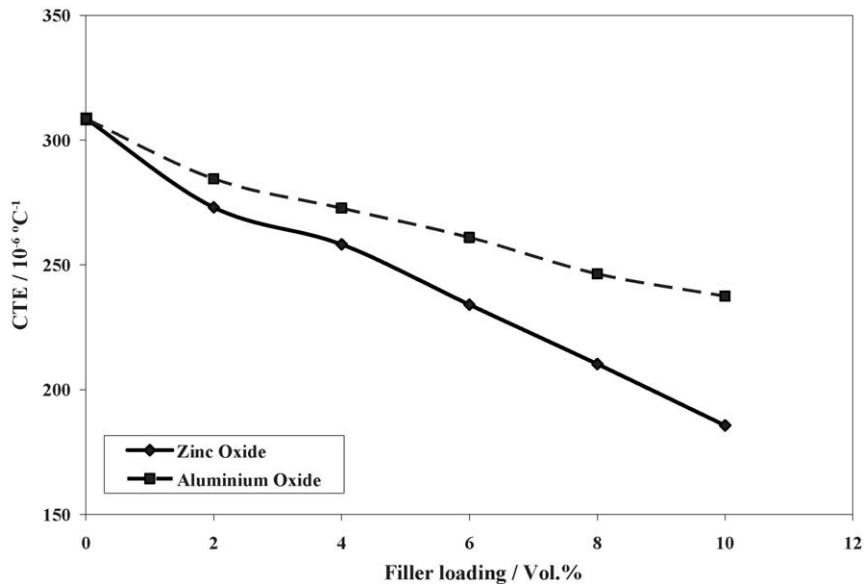


Fig. 7. Comparison between the CTE of ZnO and Al_2O_3 filled thermal pads.

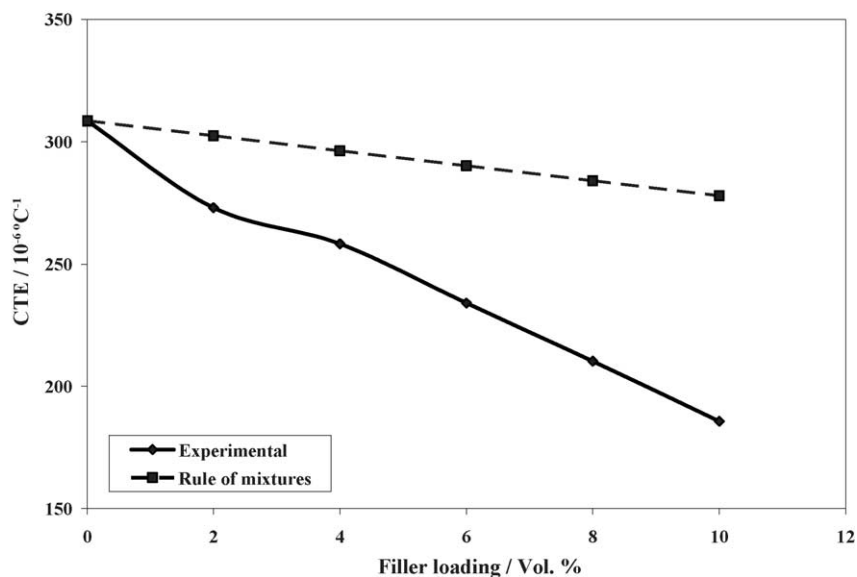


Fig. 8. Comparison of CTE of ZnO filled thermal pads with theoretical predictions.

no visible conductive chains are observed in both the thermal pads, indicating that percolation threshold has yet to be reached at 10 vol.% filler loading. However, comparison between the cross-sections of both the thermal pads showed that the Al₂O₃ fillers are more densely packed than ZnO fillers in the silicone rubber matrix, due to the larger particle size of the Al₂O₃ fillers.

3.2. Thermal stability test

Fig. 6 shows the thermogravimetric results of thermal pads filled with 10 vol.% of Al₂O₃ and ZnO fillers respectively, with an unfilled silicone rubber as a comparison. The thermal

pads were evaluated from 30 to 250 °C at 5 °C/min, which is the lower and upper limit of a device operating temperature. However, thermal pads are normally used in devices whose operating temperatures do not exceed 125 °C. From Fig. 6, the TGA curve clearly shows that the addition of fillers into the silicone rubber matrix improves its thermal stability, as at 125 °C, a relative weight loss of 1.36 wt.% was observed for the unfilled thermal pads compared to 0.77 and 0.78 wt.% for Al₂O₃ and ZnO filled thermal pads, respectively. When further heated up to 250 °C, a relative weight loss of 2.65% was observed for the unfilled thermal pads compared to 1.66% and 1.67% for Al₂O₃ and ZnO filled thermal pads, respectively. The reasons for the improvement in thermal stability of

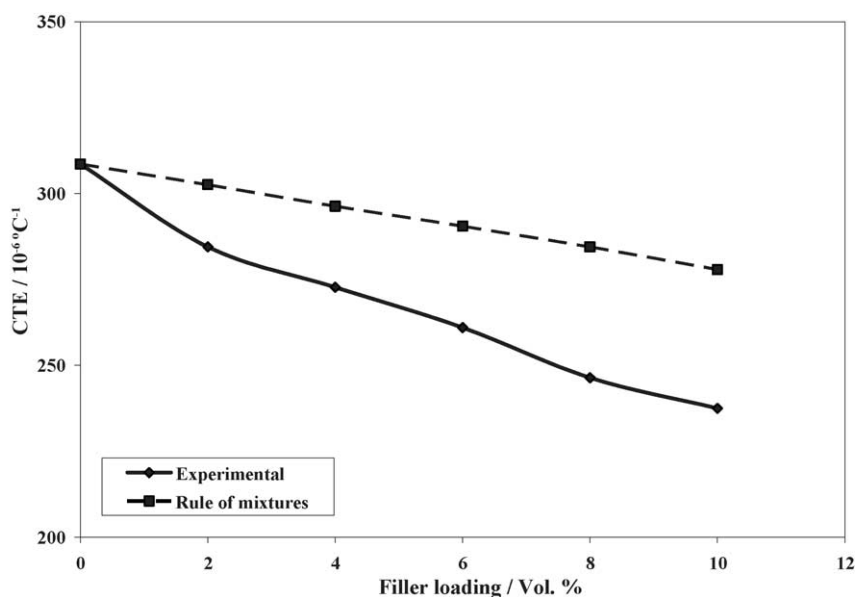


Fig. 9. Comparison of CTE of Al₂O₃ filled thermal pads with theoretical predictions.

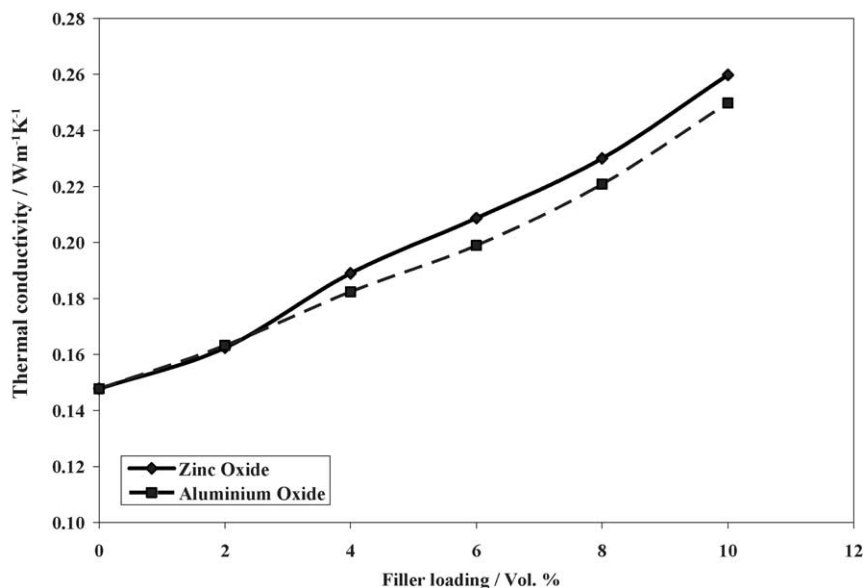


Fig. 10. Thermal conductivity of Al₂O₃ and ZnO filled thermal pads.

the filled thermal pads is probably attributed to the increase in physical and chemical cross-linking points, attributed to the interactions between the filler and silicone rubber [29]. Based on the thermogravimetric results in Fig. 6, the application of silicone rubber as thermal pads should be limited to low power devices, such as chip sets to avoid significant degradation in formulation which would reduce its thermal performance.

3.3. Coefficient of thermal expansion

From Fig. 7, a reduction in CTE was observed with increasing filler loading. For any given filler loading, ZnO filled

thermal pads have a lower CTE than Al₂O₃ filled thermal pads. This is most probably due to the lower intrinsic CTE of ZnO fillers compared to that of Al₂O₃. At a filler loading of 10 vol.%, the CTE of Al₂O₃ filled thermal pads and ZnO filled thermal pads are 237.5×10^{-6} and $185.7 \times 10^{-6} \text{ } ^\circ\text{C}^{-1}$, respectively, compared to $308.7 \times 10^{-6} \text{ } ^\circ\text{C}^{-1}$ of the unfilled thermal pads. This clearly indicates that the addition of fillers reduces the CTE of the silicone rubber matrix.

Figs. 8 and 9 show the comparison between experimental data and the theoretical model, which was based on rules of mixture for both the ZnO and Al₂O₃ filled thermal pads respectively. The equation for rules of mixture is expressed

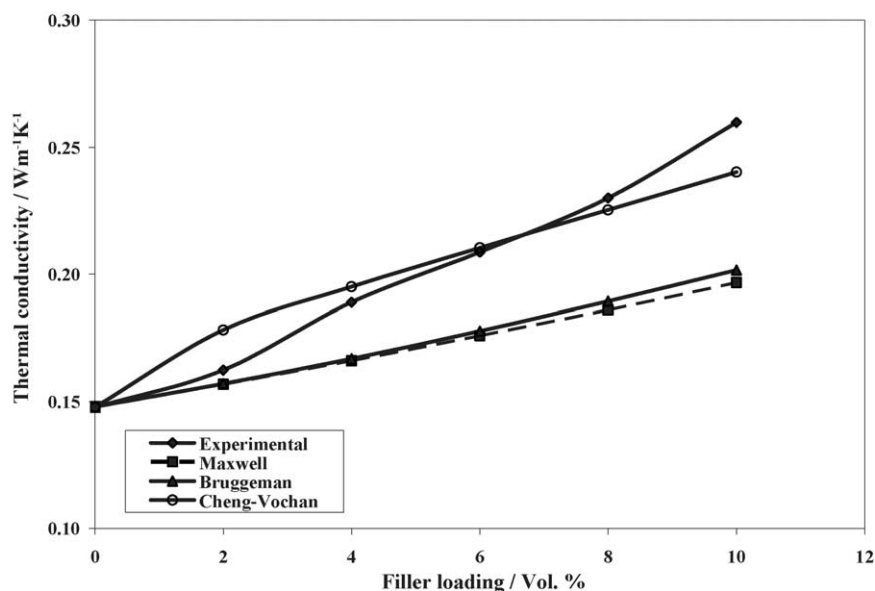


Fig. 11. Comparison of thermal conductivity of ZnO filled thermal pads with theoretical predictions.

as

$$\alpha_c = \alpha_f V_f + \alpha_m (1 - V_f) \quad (2)$$

with α_c , α_m and α_f representing the CTEs of the composite, matrix and fillers respectively and V_f the volume fraction of the fillers. From Figs. 8 and 9, it can be seen that the CTE obtained from experimental data is lower than that of the theoretical model. The reason for the deviations is because the theoretical model did not take into account the mechanical interaction between the different materials in the composite [30]. Mechanical interaction between the fillers and matrices probably binds the matrix together, thus preventing it from expanding as much as it would on its' on. Similar studies conducted by Wong et al. on polymer composites filled with ceramic fillers reported a similar observation as ours.

During temperature cycle, in which the thermal pads are subjected to a predetermined number of cycles of heating and cooling to test its reliability, thermal pads are expected to contract more than the copper heat spreader due to the CTE mismatch between the two materials. This could potentially cause deterioration in thermal performance due to increasing thermal contact resistance. Therefore, ZnO filled thermal pads are more suitable compared to Al_2O_3 filled thermal pads, due to its lower CTE at a fixed filler loading.

3.4. Thermal conductivity

Fig. 10 shows the thermal conductivity as a function of filler loading for both the Al_2O_3 and ZnO filled silicone rubber. It was observed that the thermal conductivity in both the composites increases with filler loading, whereby at a fixed filler loading, ZnO filled thermal pads, showed a higher thermal conductivity value compared to Al_2O_3 filled thermal pads. The higher thermal conductivity of ZnO filled thermal

pads is possibly due to higher intrinsic thermal conductivity of ZnO fillers ($60 \text{ W m}^{-1} \text{ K}^{-1}$) compared to Al_2O_3 fillers ($30 \text{ W m}^{-1} \text{ K}^{-1}$). In addition the finer ZnO fillers ($1 \mu\text{m}$) have a wider surface area and are more easily diffused in the polymer network compared to Al_2O_3 fillers ($10 \mu\text{m}$).

In Figs. 11 and 12, theoretical models were used to predict the thermal conductivity of the Al_2O_3 and ZnO filled thermal pads respectively. The results obtained were then compared with our experimental data. Among the theoretical models which were used to predict the thermal conductivity values are Maxwell–Eucken, Bruggeman and Cheng–Vochan model [31]. From Figs. 11 and 12, it can be observed that the predictions of the Maxwell–Eucken and Bruggeman models deviate significantly from the experimental data, while Cheng–Vochan model overestimates at filler loading less than 6 vol.% for ZnO and 8 vol.% for Al_2O_3 . The reason for the deviations is because the theoretical models did not take into account the state of filler dispersion in the composite, especially for composites with low filler content [32]. Another probable factor is because each of these models shows good agreement with experimental data, only in certain composite systems. However, by fitting our experimental data into the Agari model, a possible explanation of the state of filler dispersion in our thermal pads could be obtained:

$$\log k = V_f C_2 \log K_f + V_p \log(C_1 k_p) \quad (3)$$

In the Agari model, represented by the equation above, k represents the thermal conductivity of the thermal pads, V_f and V_p the volume fraction of fillers and polymer respectively, C_1 the crystallinity of the matrix, and finally C_2 the measure of ease for the formation of conductive chains [33–35]. According to Agari, the values of C_1 and C_2 should be in between 0 and 1. The closer C_2 values are to 1, the more easily conductive chains are formed in the composite.

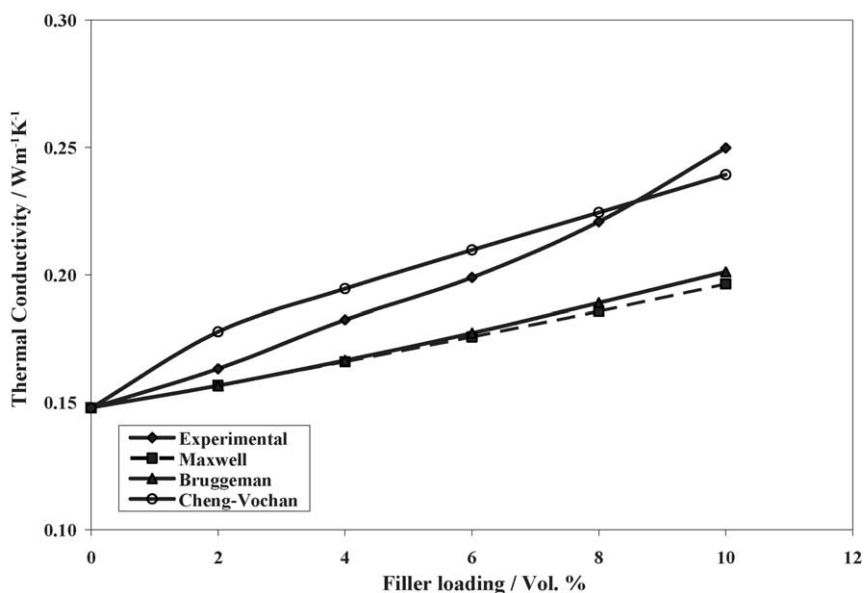


Fig. 12. Comparison of thermal conductivity of Al_2O_3 filled thermal pads with theoretical predictions.

Table 4
 C_1 and C_2 of Agari model for polymer composites

System	C_1	C_2	Thermal conductivity ($\text{Wm}^{-1} \text{K}^{-1}$) at 10 vol.%
Si rubber– Al_2O_3	0.8159	0.9647	0.2498
Si rubber–ZnO	0.8191	0.9192	0.2598

From Table 4, it is observed that the addition of Al_2O_3 or ZnO fillers into the silicone rubber matrix, affects the C_2 values more strongly than the C_1 values. This observation indicates that neither Al_2O_3 nor ZnO fillers affect the secondary structure of the silicone rubber. From Table 4 it was also observed that the C_2 values for both the thermal pads are affected by the addition of fillers, with the Al_2O_3 filled thermal pads showing a higher C_2 value compared to ZnO filled thermal pads. This is because a better state of filler dispersion is achieved in Al_2O_3 filled thermal pads compared to ZnO filled thermal pads as observed from SEM micrographs in Fig. 5(a). The higher C_2 values observed in Al_2O_3 filled thermal pads are also attributed to the larger particle size of the Al_2O_3 fillers (10 μm) which have a lower thermal contact resistance compared to the 1 μm ZnO fillers. However, values of thermal conductivity were higher for ZnO filled thermal pads owing to its higher intrinsic thermal conductivity of its fillers.

4. Conclusion

Elastomeric thermal pads were successfully prepared from silicone rubber and thermal conductive Al_2O_3 or ZnO fillers. The addition of either Al_2O_3 or ZnO fillers into the silicone rubber increases both its thermal stability and thermal conductivity but reduces its CTE. Relationship between fillers and the silicone rubber matrix obtained from the Agari model, showed that Al_2O_3 filled thermal pads have a higher likelihood for the formation of conductive chains, due to its larger particle size, as observed from SEM micrographs. Comparatively at a fixed filler loading, ZnO filled silicone rubber exhibited better thermal performance compared to Al_2O_3 filled silicone rubber, due to its higher intrinsic thermal conductivity and lower intrinsic CTE value. It's important that the application of ZnO filled silicone rubber as elastomeric thermal pads be limited to low power devices such as chip sets to avoid significant degradation, with a small pressure applied to it to ensure good conformity at the interfaces.

Acknowledgements

The authors thankfully acknowledge the research grant awarded by Intel Technologies Sdn. Bhd. One of the authors, Mr. Sim Lim Chong a recipient of Intel fellowship grant, thankfully acknowledges Intel Technologies Sdn. Bhd. for the award.

References

- [1] Y. He, B.E. Moreira, A. Overson, S.H. Nakamura, C. Bider, J.F. Briscoe, Thermal characterization of an epoxy-based underfill material for flip chip packaging, *Thermochim. Acta* 357–358 (2000) 1–8.
- [2] R. Viswanath, V. Wakharkar, A. Watwe, V. Lebonheur, Thermal performance challenges from silicone to systems, *Intel Technol. J. Q3* (2000) 1–16.
- [3] X. Yunsheng, L. Xiangcheng, D.D.L. Chung, Lithium doped polyethylene-glycol based thermal interface pastes for high contact conductance, *J. Electron. Packag.* 124 (2002) 188–191.
- [4] E.G. Wolff, D.A. Schneider, Prediction of thermal contact resistance between polished surfaces, *Int. J. Heat Mass Transfer.* 41 (1998) 3469–3482.
- [5] X. Yunsheng, L. Xiangcheng, D.D.L. Chung, Sodium silicate based thermal interface material for high thermal contact conductance, *J. Electron. Packag.* 122 (2000) 128–131.
- [6] C.K. Leong, D.D.L. Chung, Carbon black dispersions as thermal pastes that surpass solder in providing high thermal contact conductance, *Carbon* 41 (2003) 2459–2469.
- [7] Y. He, DSC and DMTA studies of a thermal interface material for packaging high speed microprocessors, *Thermochim. Acta* 392 (2002) 13–21.
- [8] J.P. Gwinn, R.L. Webb, Performance and testing of thermal interface materials, *Microelectron. J.* 34 (2003) 215–222.
- [9] C.P. Chiu, G.L. Solbrekken, V. LeBonheur, Y.E. Xu, Applications of phase-change materials in Pentium® III and Pentium® III Xeon™ Processor Cartridges, in: *Proceedings of the International Symposium on Advanced Packaging Materials*, 2000, pp. 265–270.
- [10] C.P. Chiu, B. Chandran, M. Mello, K. Kelley, An accelerated reliability test method to predict thermal grease pump out in flip chip applications, in: *Proceedings of the Electronic Components and Technology Conference*, 2001.
- [11] R.S. Prasher, Surface chemistry and characteristics based model for the thermal contact resistance of fluidic interstitial thermal interface materials, *J. Heat Transfer.* 123 (2001) 969–975.
- [12] C.P. Chiu, G.L. Solbrekken, T.M. Young, Thermal modeling and experimental validation of thermal interface performance between non flat surfaces, in: *Proceedings of the Inter Society Conference on Thermal Phenomena*, 2000, pp. 55–62.
- [13] C.P. Chiu, G.L. Solbrekken, T.D. Chung, Thermal modeling of grease type interface material in PPGA application, in: *Proceedings of the 13th IEEE SEMI-THERM Symposium*, 1997, pp. 57–63.
- [14] C.P. Chiu, G.L. Solbrekken, V. LeBonheur, Y.E. Xu, Applications of phase-change materials in Pentium® III and Pentium® III Xeon™ Processor Cartridges, in: *Proceedings of the International Symposium on Advanced Packaging Materials*, 2000, pp. 265–270.
- [15] Y. Xu, D.D.L. Chung, C. Mroz, Thermally conducting aluminum nitride polymer-matrix composites, *Compos. Part A* 32 (2001) 1749–1757.
- [16] S. Yu, P. Hing, X. Hu, Thermal Conductivity of polystyrene-aluminum nitride composites, *Compos. Part A* 33 (2002) 289–292.
- [17] S. Rimdusit, H. Ishida, Development of new class of electronic packaging materials based on ternary systems of benzoxazine, epoxy, and phenolic resins, *Polymers* 41 (2000) 7941–7949.
- [18] D.D.L. Chung, Thermal Interface Materials, *J. Mater. Eng. Perform.* 10 (2001) 56–59.
- [19] R.L. Webb, J.P. Gwinn, Low melting point interface material, in: *Proceedings of the Inter Society Conference on Thermal Phenomena*, IEEE, 2002, pp. 671–676.
- [20] A.A. Basfar, Hardness measurement of silicone rubber and polyurethane rubber cured by ionizing measurement, *Radiat. Phys. Chem.* 50 (6) (1997) 607–610.
- [21] Q.G. Gu, Q.L. Zhou, Preparation of high strength and optically transparent silicone rubber, *Eur. Polym. J.* 34 (11) (1998) 1727–1733.

- [22] L.X. Zhang, S.Y. He, Z. Xu, Q. Wei, Damage effects and mechanism of proton irradiation on methyl silicone rubber, *Mater. Chem. Phys.* 83 (2004) 255–259.
- [23] Y. Tang, R. Tsiang, Rheological, extractive and thermal studies of the room temperature vulcanized polydimethylsiloxanes, *Polymer* 40 (1999) 6135–6146.
- [24] American Society for Testing Materials, method D3184-98 (1998).
- [25] American Society for Testing Materials, method D5470-98 (1998).
- [26] J.P. Gwinn, M. Saini, R.L. Webb, Apparatus for accurate measurement of interface resistance of high performance thermal interface materials, in: *Proceedings of the Intersociety Conference on Thermal Phenomena*, IEEE, 2000, pp. 644–650.
- [27] A. Devpura, P.E. Phelan, R.S. Prasher, Percolation theory applied to the analysis of thermal interface materials in flip-chip technology, in: *Proceedings of the Inter Society Conference on Thermal Phenomena*, 2000, pp. 21–28.
- [28] P.E. Phelan, R.C. Niemann, Effective thermal conductivity of thin, randomly oriented composite material, *J. Heat Transfer.* 120 (1998) 971–976.
- [29] J. Zhang, S. Feng, Q. Ma, Kinetics of the thermal degradation and thermal stability of conductive silicone rubber filled with conductive carbon black, *J. Appl. Polym. Sci.* 89 (2003) 1548–1554.
- [30] C.P. Wong, R.S. Bollampally, Thermal conductivity, elastic modulus and coefficient of thermal expansion of polymer composites filled with ceramic particles for electronic packaging, *J. Appl. Polym. Sci.* 74 (1999) 3396–3403.
- [31] F. Lin, G.S. Bahtia, J.D. Ford, Thermal conductivities of powder filled epoxy resins, *J. Appl. Polym. Sci.* 49 (1993) 1901–1908.
- [32] S. Yu, P. Hing, X. Hu, Thermal conductivity of polystyrene-aluminum nitride composite, *Compos. Part A* 33 (2002) 289–292.
- [33] X. Lu, G. Xu, Thermal conductive polymer composites for electronic packaging, *J. Appl. Polym. Sci.* 65 (1997) 2733–2738.
- [34] Y. Agari, T. Uno, Estimation on thermal conductivities of filled polymers, *J. Appl. Polym. Sci.* 32 (1986) 5705–5712.
- [35] Y. Agari, A. Ueda, S. Nagai, Thermal conductivities of composites in several types of dispersion systems, *J. Appl. Polym. Sci.* 65 (1997) 2733–2738.